Self-driven propagation of crack arrays: A stationary two-dimensional model

Thomas Boeck
Center for Physical Fluid Dynamics, Department of Mechanical Engineering, Dresden University of Technology, 01062 Dresden, Germany

Hans-Achim Bahr
Institute for Solid Mechanics, Department of Mechanical Engineering, Dresden University of Technology, 01062 Dresden, Germany

Stefan Lampenscherf
Institute for Materials Science, Department of Mechanical Engineering, Dresden University of Technology, 01062 Dresden, Germany

Ute Bahr
Institute for Theoretical Physics, Department of Physics, Dresden University of Technology, 01062 Dresden, Germany
(Received 29 July 1998)

Heat or mass transfer across crack surfaces can generate localized shrinkage causing internal stresses which drive crack propagation. We present experiments suggesting the existence of such a diffusion controlled directional self-cracking. We formulate a simple two-dimensional stationary model of straight, evenly spaced, parallel cracks for this process, which takes into account the heat transfer across the crack surfaces and the interaction of neighboring cracks. The governing equations are solved numerically using finite elements. Crack spacing and velocity can be predicted utilizing a stability argument combined with simple ideas about the formation of the crack array. The selected solution is marginally stable with minimal values for crack spacing and velocity. The results are compared with predictions from a simpler model by Yakobson. [S1063-651X(99)00702-3]

PACS number(s): 46.50.+a, 62.20.Mk, 81.40.Np, 44.30.+v

I. INTRODUCTION

Crack patterns are frequently encountered in everyday life as a result of drying up of soil, wood, paint, etc. In some cases, these patterns are fairly similar, e.g., patterns on old paintings or stove tiles resemble those emerging after quenching a heated ceramic slab [1]. The common cause of all crack structures is tensile stress due to shrinkage within a limited region of the material. It is of secondary importance whether the shrinkage is caused by drying, quenching, relocation processes, chemical reactions, etc.

The variety of different crack patterns is remarkable. In directional crack propagation, netlike patterns (Fig. 1) and periodic arrays of parallel cracks of equal (Fig. 2) or hierarchically ordered length [1] are observed. Instead of straight cracks, periodically or chaotically oscillating cracks are also possible [2]. This variety results from the interaction between the cracks themselves and between the cracks and the outer boundaries of the material.

For simple crack configurations, the generation of crack patterns can be modeled using methods from linear-elastic fracture mechanics and bifurcation theory. In this way, the morphological transitions between straight and oscillatory motion for single and multiple cracks, which were observed in an ingeniously simple experiment by Yuse and Sano [3], could be explained theoretically [4–8]. The advantage of this experiment, in which a heated glass strip is lowered into cold water at constant velocity, consists in the controlled, stationary crack propagation over a wide range of velocities.

The transition from a regular to a hierarchically ordered array of parallel cracks was investigated in [1,8]. In this problem, cracks move due to thermal stresses generated by the quenching of a heated ceramic slab. The initially short and densely spaced cracks experience an increasing mutual unloading effect as they grow from the surface into the interior of the slab. As a consequence, some of the cracks suddenly stop growing, which leads to the hierarchical order.

The same mechanism is also important for geothermal energy extraction by pumping cold water through warm rock [9,10]. The deeper and wider the generated cracks reach, the more geothermal heat can be extracted.

In the late stage of this process it appears possible that the heat is mainly transferred across the surfaces of secondary cracks and not across the surface of the primary fissures. These secondary cracks can move due to the thermal stresses they generate by extracting heat from the rock. For this situation, Weiss (see [11]) suggested that crack propagation could become stationary without differentiation in crack length. We shall refer to this process as self-cracking to emphasize the temporal evolution involved.

The existence of stationary directional self-cracking due to shrinkage by chemical decomposition was assumed by Yakobson [12], who analyzed a one-dimensional model. In his work, the term self-fracturing is used for this process. Mass transfer across the crack surfaces is treated in a one-dimensional approximation and the interaction between neighboring cracks is ignored. In simple laboratory experiments the shrinkage can be easily produced by drying of fluid precursors, monolayers of microspheres or gels [13–15].

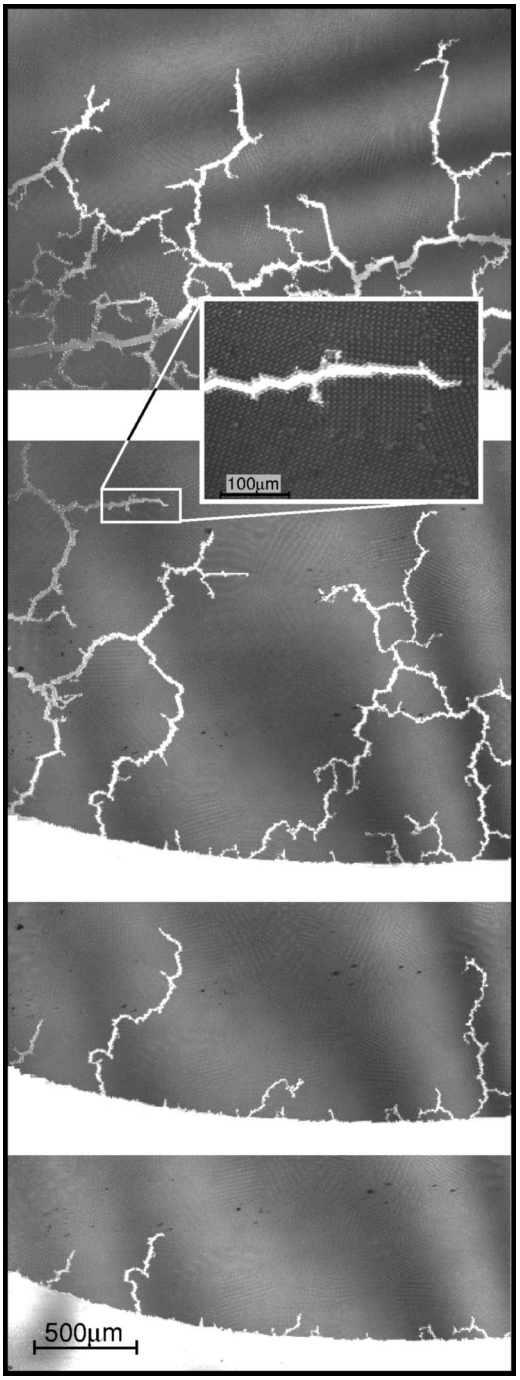

FIG. 1. Evolution of a crack pattern in a drying monolayer of uniformly sized microspheres confined between two glass plates. Drying connected with shrinking of the spheres happens only from one open lateral edge and causes directional cracking. The two-dimensional cracks can open relatively freely because of weak bonding of the microspheres to the glass surface (see inset). The lower three photographs show three transient stages of cracking from the boundary of the monolayer. The upper photograph shows the late stage of cracking with precursor cracks in front of the moving crack boundary corresponding to the model of Yakobson.

In the experiments reported below we have observed net-like crack patterns as well as arrays of parallel cracks. These experiments have led us to an extended two-dimensional model for such self-cracking processes. It incorporates interaction of neighboring cracks which determines the lateral crack spacing.

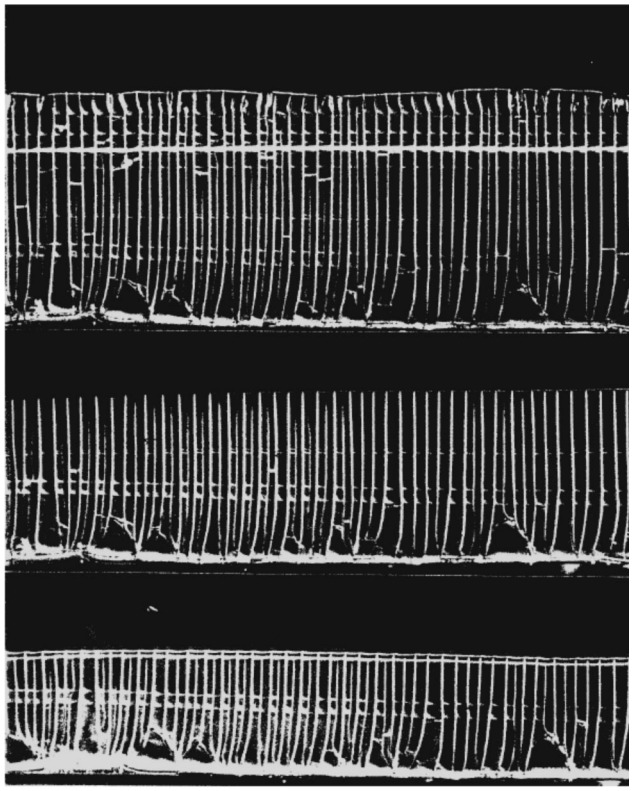

FIG. 2. Evolution of a regular array of straight parallel cracks resulting from directional drying of fluid ceramic precursor between two glass plates: photographs taken after 10, 15, 20 min. The tunneling cracks are three dimensional because they do not open at the bounding glass plates. The crack spacings scale with the precursor thickness of 0.05 mm.

The paper is organized as follows. Experimental results are presented in the following section. In Sec. III we formulate a theoretical model for self-cracking. Our formulation assumes that cooling and thus thermal stresses drive the cracks, but it is mathematically equivalent to the cases of chemical decomposition or drying [11]. The numerical method and results are presented in Sec. IV. Next, crack spacings and velocities are computed as functions of the material properties, heat transfer coefficient, and the temperature difference between coolant and the fracturing material. Finally, we compare our findings with the results of the one-dimensional model by Yakobson [12] and indicate possible directions of future work.

II. DIRECTIONAL DRYING EXPERIMENTS

In the following we describe two experiments on directional drying. It must be mentioned that they do not directly relate to the model to be presented in Sec. III. Instead, we select typical features realized either in one or in the other experiment in order to obtain a minimal theoretical model.

Figure 1 shows the evolution of a two-dimensional crack pattern in a drying monolayer of uniformly sized microspheres confined between two parallel glass plates glued at the edges. In contrast to the experiments by Skjeltorp and

Meakin [14], the water is removed only across one open lateral edge, which causes directional cracking from this edge into the material. Furthermore, no additional cracks appear in the interior of the sample. The polymer microspheres adhere more strongly among each other than to the glass plates. Therefore the cracks can open relatively freely also at the glass surfaces, and the monolayer opens up completely. The drying front slowly moves into the monolayer, and the cracks grow accordingly. Because of mutual unloading, cracks can temporarily be left behind. Straight crack propagation is only observed within single grains of the polycrystalline monolayer. They are deflected at grain boundaries (see inset). Cracks can merge and can even grow in the direction opposite to the drying front. Resumed growth of formerly stopped cracks is also found. The late stage of cracking (top) shows precursor cracks in front of the moving crack boundary corresponding to the model of Yakobson [12].

The evolution of a regular array of parallel cracks is shown in Fig. 2. In analogy to the experiments by Allain and Limat [13], fluid ceramic precursor (chrome-acetate in water) was placed between two glass plates and dried at a temperature of 80 °C. In the central region, cracks are left behind in an alternating pattern as previously found in thermal cracking. In contrast to Fig. 1, these cracks do not open at the glass plates. They represent three-dimensional cracks which are called tunneling cracks [16].

Before attempting a fully three-dimensional crack modeling under inhomogeneous loading it seems more appropriate to investigate simpler two-dimensional models such as the one studied in this paper. It contains the additional assumption of stationary self-cracking. Experiments supporting this assumption have been undertaken with a different system [15].

III. TWO-DIMENSIONAL MODEL FOR SELF-CRACKING

A. Basic equations

In the formulation of our two-dimensional model of diffusion controlled, directional self-cracking we consider thermal stresses as the driving mechanism for crack motion. We also assume that the cooling of the fracturing material is mediated by the crack surfaces. The boundary conditions for the temperature distribution in the material therefore depend on the position of the moving cracks, i.e., the problem involves moving boundaries. In the basic analysis of such problems one usually considers stationary solutions. This approach reduces the problem to one with fixed boundaries in a moving frame of reference. Moreover, it is generally assumed that the stationary solutions represent asymptotical states.

We consider a uniform array of evenly spaced, parallel cracks as shown in Fig. 3, which extend indefinitely in the z direction. The cracks are moving with constant velocity v in positive x direction. The lateral spacing of the cracks is $2p$, and we assume that the cracks extend from $x=-\infty$ to $x=0$. In the half space far ahead of the cracks (large positive values of x), the temperature field T is uniform at T_0, and stresses and displacements vanish. The temperature distribution is governed by the ordinary heat diffusion equation with constant thermal diffusivity κ, which reads

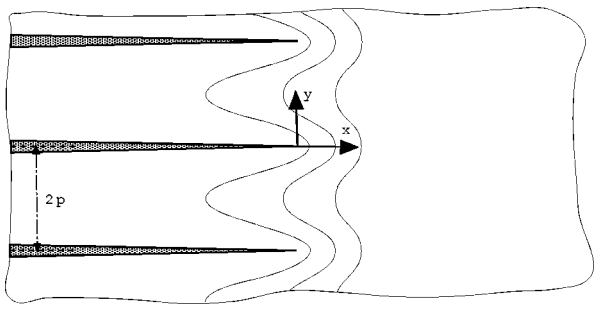

FIG. 3. Isotherms for a periodic array of parallel cracks moving with constant velocity in x direction (schematic illustration). Crack spacing and crack length are uniform. The cracks extend indefinitely in z direction.

$$\kappa\nabla^2 T(x,y)+v\frac{\partial}{\partial x}T(x,y)=0 \tag{1}$$

in the frame of reference moving with the cracks. The cracks are assumed to be in mechanical equilibrium with respect to the given temperature distribution. We consider the case of plane strain. The equilibrium condition [17]

$$\sum_{j=x,y}\frac{\partial\sigma_{ij}}{\partial x_j}=0 \tag{2}$$

holds for $i=x,y$ in both the fixed and moving frames of reference. The stress tensor is given by

$$\sigma_{ij}=-\frac{E}{1-2\nu}\alpha(T-T_0)\delta_{ij}+\frac{E}{1+\nu}\left(u_{ij}+\frac{\nu}{1-2\nu}\delta_{ij}\sum_{l=x,y}u_{ll}\right), \tag{3}$$

where $u_{ij}=(\partial_i u_j+\partial_j u_i)/2$ represents the deformation tensor, u_x, u_y denote the displacement fields, and T_0 refers to the reference state. The other symbols α, E, ν denote thermal expansion coefficient, Young's modulus, and Poisson number.

The basic equations must be complemented by two mechanical and one thermal boundary condition on the domain boundaries. Because of symmetry we only need to consider a domain of width p adjacent to a crack. For this domain, we choose the coordinate axes such that the crack surface coincides with the negative x axis. Symmetry implies that $\sigma_{xy}=0$ on the entire x axis and on the line $y=p$. The normal stress σ_{yy} vanishes on the crack surface. The undeformed half space ahead of the cracks ensures that the displacement u_y vanishes for $y=p$ and for $y=0,\ x>0$. The stresses also vanish in the half space for $x\to\infty$. Figure 4 (top) summarizes the mechanical boundary conditions.

For the thermal problem, symmetry requires that $\partial_y T=0$ for $y=p$ and for $y=0,\ x>0$. We assume that the heat flux density $-\lambda\partial_y T$ on the crack surface is given by Newton's law of cooling

$$\lambda\partial_y T(x,y=0)=h[T(x,y=0)-T_1]. \tag{4}$$

In this equation, the heat conductivity λ and the heat transfer coefficient h appear as additional parameters. The temperature $T_1<T_0$ is maintained outside the material in the interior

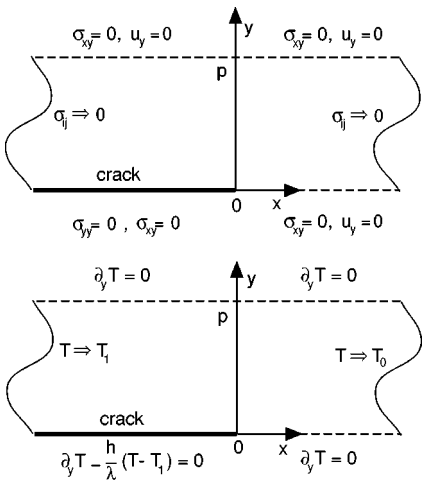

FIG. 4. Mechanical (top) and thermal (bottom) boundary conditions.

of the crack. It could be regarded as the temperature of the coolant. A summary of the thermal boundary conditions is given in Fig. 4 (bottom).

The basic equations and boundary conditions in the moving frame of reference are now completely specified. With the material properties, the temperatures T_0, T_1, crack distance p, and velocity v given, we can compute the stress and temperature field in the entire domain. However, crack motion is possible only if the elastic energy released by advancing the crack can balance the fracture energy needed for creation of new material surface. This is expressed by the condition

$$G dA \geqslant G_c dA, \tag{5}$$

where $G dA$ denotes the amount of elastic energy released in creating new crack surface dA, and $G_c dA$ represents the fracture energy needed for generating dA. Steady crack motion is only possible for

$$G = G_c . \tag{6}$$

Otherwise mechanical equilibrium is not maintained in advancing the crack. We remark that the energy release rate G is a quadratic functional of the stress field.

The crack propagation condition (6) implies that p and v cannot be arbitrarily chosen, but must satisfy a functional relation. Nevertheless, there is still a one-dimensional manifold of stationary solutions. However, since neither p nor v are externally controlled quantities, there should be another scalar relation which selects one particular value of v and p. As in other moving boundary problems, such a condition may be obtained by studying the stability of the stationary solution.

B. Stability of a uniform array of cracks

In the stationary state, the crack array must be stable with respect to perturbations. However, the analysis of even the simplest perturbations is a difficult problem in the framework of our simple mathematical model. We will therefore consider only a small class of perturbations, namely, perturbations without directional deviations where every second crack is of equal length. These perturbations will be referred to as 2-periodic. This implies that the cracks are constrained to moving along straight lines. The restriction to 2-periodic perturbations seems justified in the light of the analysis of crack pattern formation in the quenched ceramic slab. In this problem it turns out that these perturbations are the first to become unstable [1].

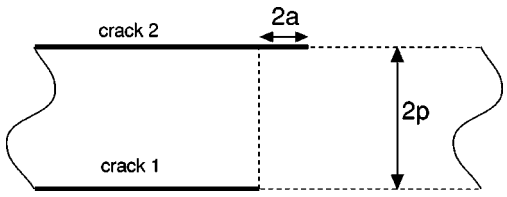

FIG. 5. 2-periodic disturbance in crack length.

Usually, a stability computation will proceed by a linearization about the basic state. However, the crack motion in our problem is not described by a differential equation. We have not been able to devise an analytical approach for a stability calculation.

In the following, we shall propose the so-called quasistatic stability criterion. We consider this criterion as necessary and sufficient to ensure stability for the above class of perturbations. A formal mathematical derivation of this criterion remains an open problem.

For our stability considerations we assume that every second crack starts to move faster whereas the remaining ones do either reduce their speed or even stop moving. Given the positions of the crack tips as a function of time, we can compute the temperature fields and the energy release rates for each crack. Instability may occur if the crack propagation condition acts in favor of a differentiation in crack length, i.e., if $G \geqslant G_c$ for the faster crack and $G \leqslant G_c$ for the slower crack in the course of the fictitious motion. Clearly, this definition of instability contains all of the unstable motions that are physically allowed. However, checking for stability still requires consideration of an infinite variety of fictitious crack motions. The most unstable of them must be identified to obtain a workable stability criterion.

The faster crack is affected by two mechanisms acting in opposite directions. The first effect is a purely geometrical unloading effect. The advanced crack gets a larger share of the elastic energy to be released than the crack remaining behind. One could equally say that the advanced crack experiences a reduced shielding from its neighbors. This mechanism represents the driving force of instability in this system.

The counteracting thermal effect is due to the fact that the crack tip is surrounded by comparatively warmer material giving rise to a lower energy release rate than for slower advancement. This effect will decrease as the relative motion between the cracks is reduced, whereas the geometrical unloading effect is not directly related to the crack speed. As a result, the most favorable situation for instability appears to be a quasistatic change in crack length, in which the thermal stresses have sufficient time to build up near the tip of the faster crack.

We are now in a position to formulate the quasistatic stability criterion in mathematical terms. Consider a 2-periodic disturbance in crack length as shown in Fig. 5. The difference in crack length between cracks 1 and 2 is denoted by

$2a$, where a can be positive or negative. Let us also assume that temperature field satisfies the stationary heat equation (1). The energy release rates G_1 of the advanced crack and G_2 of the delayed crack differ from the value G in the uniform state. Stationarity and symmetry with respect to interchanging the crack numbering and replacing a by $-a$ imply the relation $G_1(a)=G_2(-a)$. The crack array will be quasistatically stable if G_1 does not increase with a, i.e., if

$$F=\left.\frac{dG_1}{da}\right|_{a=0}\leqslant 0. \tag{7}$$

In our problem, we expect that the shielding effect will be weak for large crack spacing. The system should then be stable. Instability may occur when the crack spacing is small. We further remark that the condition (7) can also be obtained by considering the sum of elastic energy and crack surface energy as a function of the crack tip positions and requiring that this function be minimal for $a=0$.

IV. NUMERICAL SOLUTION

The computation of the stable stationary solutions for our model comprises the following tasks. Given the material properties, the temperature difference $T_0-T_1>0$, the velocity v, and the crack spacing p we can successively compute the temperature and the stress distribution, from which the energy release rate G follows. For determination of F, the computations must be carried out for at least one configuration with cracks of different length. The number of parameters can be reduced by nondimensionalization.

A. Temperature distribution

We choose p as length scale, $\Delta T=(T_0-T_1)$ as the scale for the temperature, and shift the origin of the temperature scale to T_1. The dimensionless heat equation then reads

$$\nabla^2 T+\mathrm{Pe}\,\partial_x T=0,\quad \mathrm{Pe}=\frac{vp}{\kappa}, \tag{8}$$

where Pe denotes the Péclet number. Similarly, the nontrivial boundary condition on the crack surface becomes

$$\partial_y T=\mathrm{Bi}\,T,\quad \mathrm{Bi}=\frac{hp}{\lambda}, \tag{9}$$

where Bi is called the Biot number. The temperature distributions for given Pe and Bi have been computed numerically using the finite element package MARC [18]. Isotherms for several values of Pe and Bi are shown in Fig. 6. They are in excellent agreement with an analytical solution obtained by the Wiener-Hopf method [19]. By increasing Pe, convective heat transport becomes more important, and steeper temperature gradients build up. Correspondingly, the isotherms penetrate deeper into the region between the cracks.

The heat loss from the material across the crack surface into the coolant is affected by the Biot number. For large Biot number, the amount of heat transferred into the coolant is mainly limited by heat transport inside the material. In particular, for $\mathrm{Bi}\to\infty$, the heat flux density can increase without limit. Conversely, for small Bi the limited heat transport across the interface determines the heat losses. In summary, increasing Pe with Bi fixed heats up the region in between the cracks, whereas increasing Bi with Pe fixed cools it down. Since the load on the cracks is related to the thermal stresses due to cooling, the energy release rate should increase with Bi and decrease with Pe.

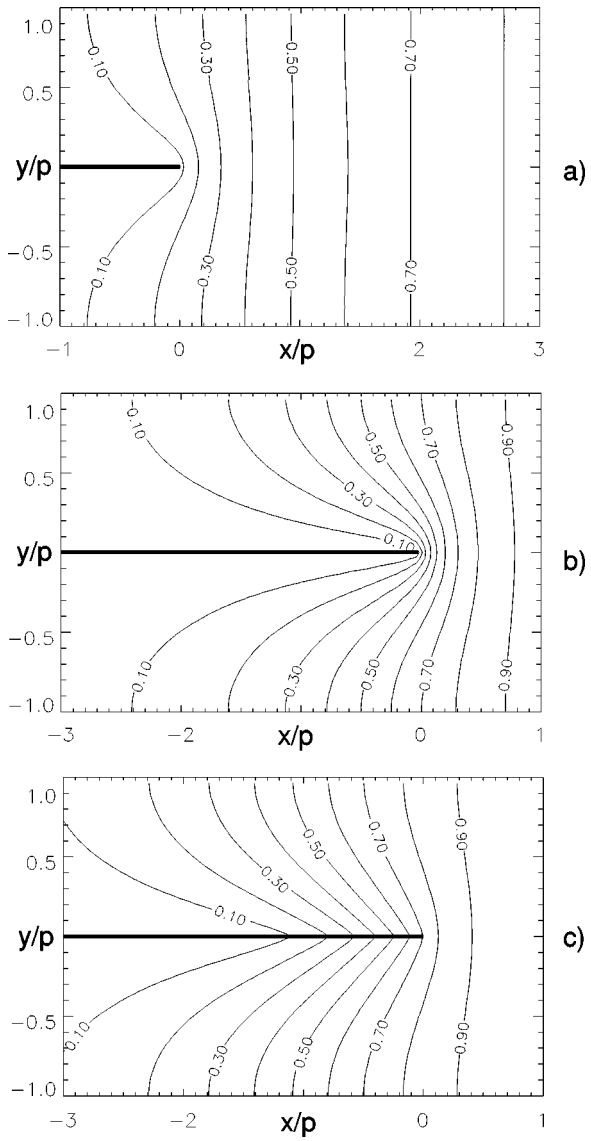

FIG. 6. Isotherms $(T-T_1)/\Delta T$ in the (x,y) plane for different values of the Péclet number Pe and the Biot number Bi: (a) $\mathrm{Bi}=\infty, \mathrm{Pe}=0.5$, (b) $\mathrm{Bi}=\infty, \mathrm{Pe}=2$, (c) $\mathrm{Bi}=1, \mathrm{Pe}=2$.

B. Energy release rate

From a simple dimensional argument it follows that the energy release rate G in our problem is of the form

$$G=\frac{1+\nu}{1-\nu}E(\alpha\Delta T)^2 p\, g(\mathrm{Pe},\mathrm{Bi}). \tag{10}$$

The ν dependence is derived in the Appendix. The function $g(\mathrm{Pe},\mathrm{Bi})$ is referred to as the normalized energy release rate.

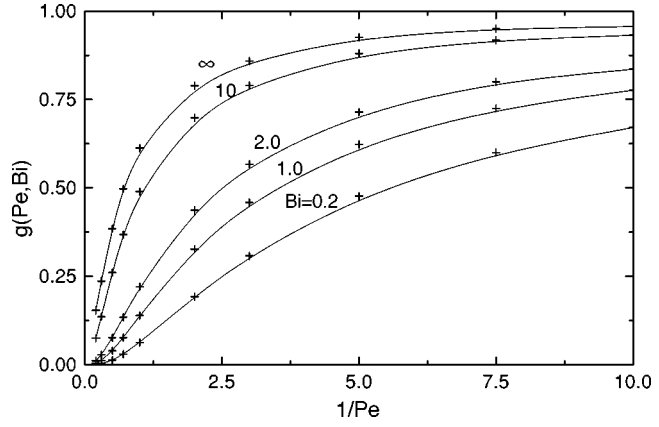

FIG. 7. Normalized energy release rate (10) for the parallel crack array of Fig. 3 as a function of the inverse Péclet number 1/Pe and Biot number Bi.

Only $g(\mathrm{Pe},\mathrm{Bi})$ has to be computed numerically since the dependence of G on the other parameters follows from Eq. (10).

The numerical evaluation of g requires the solution of Eqs. (2) and (3) for the plane strain thermal stress problem. We have again used the MARC finite element code for this purpose. The code evaluates G on the basis of integral theorems for the energy flux to the crack tip [18]. The results of our numerous computations are summarized in Fig. 7, where g is shown as a function of Pe for several fixed values of Bi. We will now explain the qualitative behavior of g in certain limiting cases of large and small Pe and Bi using some simple ideas about the temperature distribution.

We first consider the case of $\mathrm{Pe}\to 0$ and keep Bi finite. For small Pe, the cracks advance so slowly that heat diffusion reduces the temperature to the temperature of the coolant also far ahead of the cracks. Because of the presence of the large heated half space, the cooled region cannot shrink, which causes homogeneous equibiaxial stress

$$\sigma_0 = -\frac{E\alpha\Delta T}{1-\nu}. \tag{11}$$

Increasing the crack surface by dA unloads a volume of $2p\,dA$ per crack. Analogous to [20], the elastic energy density associated with the equibiaxial stress is given by $(1-\nu)\sigma_0^2/E$. After unloading with respect to the y direction the plane strain constraint in z direction leaves a residual stress $\sigma_{zz}=(1-\nu)\sigma_0$ in the unloaded region. The released energy per unit area therefore reads

$$G=\frac{2p}{E}\left[(1-\nu)\sigma_0^2-\frac{\sigma_{zz}^2}{2}\right]=\frac{1+\nu}{1-\nu}E(\alpha\Delta T)^2 p, \tag{12}$$

which corresponds to $g\to 1$. Since $\mathrm{Pe}\to 0$ generates the largest load on the cracks, g cannot become larger than unity.

Let us now consider the case of large Pe and infinite Bi, i.e., the temperature on the crack surface is now prescribed, and convection dominates over heat diffusion. In this case, the crack surface is surrounded by a thermal boundary layer, in which the temperature drops from unity to zero. Since thermal stresses opening the crack are generated only in this narrow layer, the crack spacing p is no longer relevant for the size of G. Instead, G should become proportional to the diffusion length κ/v, which is the single remaining length scale. This argument implies $g\propto 1/\mathrm{Pe}$. Our computations show that $g=0.81/\mathrm{Pe}$ in this case. We remark that this result need not hold for moderate Bi since the limited heat transfer on the crack surface reduces the thermal stresses that are acting near the crack tip.

Another interesting case is that of $\mathrm{Bi}\ll\mathrm{Pe}\ll 1$. The smallness of Bi allows the temperature field to penetrate far between the cracks, which can be seen by extrapolating the trend shown in Fig. 6. Due to the low crack velocity, the convective term can be approximately disregarded. A linear profile with respect to x which is independent of y then represents a simple approximation to the temperature distribution between the cracks. The slope of this profile is characterized by a length scale $L_h\propto 1/B$ over which the temperature decays from unity to zero. (This relation can be obtained from an energy balance for stationary crack motion. It reads $2pv\rho c\Delta T=L_h h\Delta T$ in dimensional units with the heat capacity $\rho c=\lambda/\kappa$.) Because of the mutual unloading of the cracks, only the temperature drop from unity over a fixed length of order p determines the thermal stresses relevant for the energy release rate. These stresses are of order Bi, which implies $g\propto \mathrm{Bi}^2$ [21]. Notice that this result does not contradict the earlier claim that $g\to 1$ for $\mathrm{Pe}\to 0$. It demonstrates that the origin in the (Pe,Bi) plane is a singular point.

C. Stability condition

The nondimensional form of F is similar to that of G. The stability condition (7) becomes

$$F=\frac{1+\nu}{1-\nu}E(\alpha\Delta T)^2 f(\mathrm{Pe},\mathrm{Bi})\leqslant 0, \tag{13}$$

where f depends on Pe and Bi only. We need therefore only consider the parameters Pe and Bi in the numerics. In order to compute the derivative F, we need to know the energy release rate G_1 for the advanced crack, which is ahead of the delayed crack by the distance $2a$ (cf. Fig. 5). The computational domain must therefore be extended to the full strip enclosed by two neighboring cracks since symmetry about the midplane between the cracks is lost. To compute F, we introduce small displacements a of the order of $0.01p$ and compute $G_1(a)$ in addition to G for the uniform cracks. The dimensionless quantity f is obtained by finite differences. As in the previous computations for T and g we have carefully verified our results by using finite element meshes of different length and grid spacing.

Figure 8 contains the results of the stability computations. It shows regions of stable and unstable crack propagation in the (Pe,Bi) plane separated by the stability curve Pe(Bi) computed from the quasistatic stability criterion (7) at the stability limit.

Not surprisingly, it turns out that solutions with small Pe are unstable and solutions with large Pe are stable. For large Pe, the decrease in thermal stresses acting on the advanced

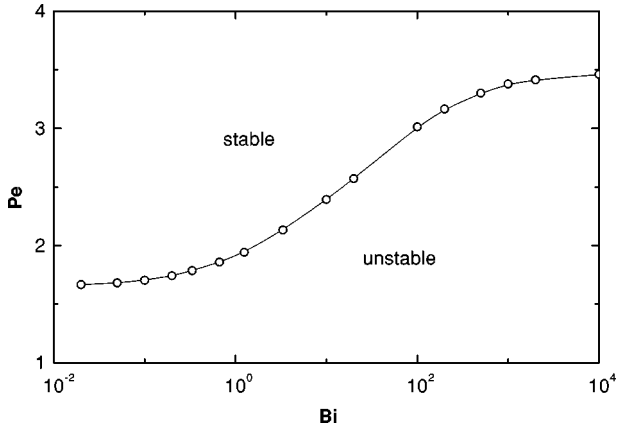

FIG. 8. Regions of stable and unstable crack propagation as a function of Péclet and Biot number. The transition line corresponds to the marginal stability condition $f(\mathrm{Pe},\mathrm{Bi})=0$.

crack is more pronounced than for small Pe, i.e., the stabilizing thermal effect is stronger for large values of Pe.

V. CRACK SPACING AND VELOCITY

We are now in a position to determine the crack velocity v and spacing p from the material properties E, α, ν, G_c, and the temperature difference $\Delta T = T_0 - T_1$. Using Eq. (10), the crack propagation condition (6) can be written as

$$g(\mathrm{Pe},\mathrm{Bi}) = \frac{l_0}{p}, \quad l_0 = \frac{G_c(1-\nu)}{(1+\nu)E(\alpha\Delta T)^2}. \tag{14}$$

The characteristic length l_0 represents the ratio of specific fracture energy and maximal thermoelastic energy density. From Eq. (13) we obtain the second condition

$$f(\mathrm{Pe},\mathrm{Bi}) \leqslant 0 \tag{15}$$

for determination of the two unknowns v and p.

The stability curves shown in Fig. 9 separate regions of stable and unstable crack spacings and crack velocities as a function of the external loading parameter hl_0/λ. This parameter contains both the temperature difference ΔT and the heat transfer coefficient h. With increasing values of h, the cooling becomes more efficient, which allows for smaller crack spacings and higher velocities.

We shall now derive the asymptotics of the stability curves for small and large hl_0/λ. From $g \propto \mathrm{Bi}^2$ and the finite limit of the critical Péclet number for $\mathrm{Bi} \to 0$ it follows that

$$\frac{p}{l_0} \propto \left(\frac{hl_0}{\lambda}\right)^{-2/3}, \quad \frac{v l_0}{\kappa} \propto \left(\frac{hl_0}{\lambda}\right)^{2/3}, \tag{16}$$

in the limit $hl_0/\lambda \to 0$. Notice that Bi tends to zero with hl_0/λ although the crack spacing p diverges in this limit. In the limit $hl_0/\lambda \to \infty$ we find that p and v approach constant values since g and the critical Péclet number become constant as $\mathrm{Bi} \to \infty$. Our numerical computations (cf. Fig. 9) show that

$$\frac{p}{l_0} \to 4.3, \quad \frac{v l_0}{\kappa} \to 0.81. \tag{17}$$

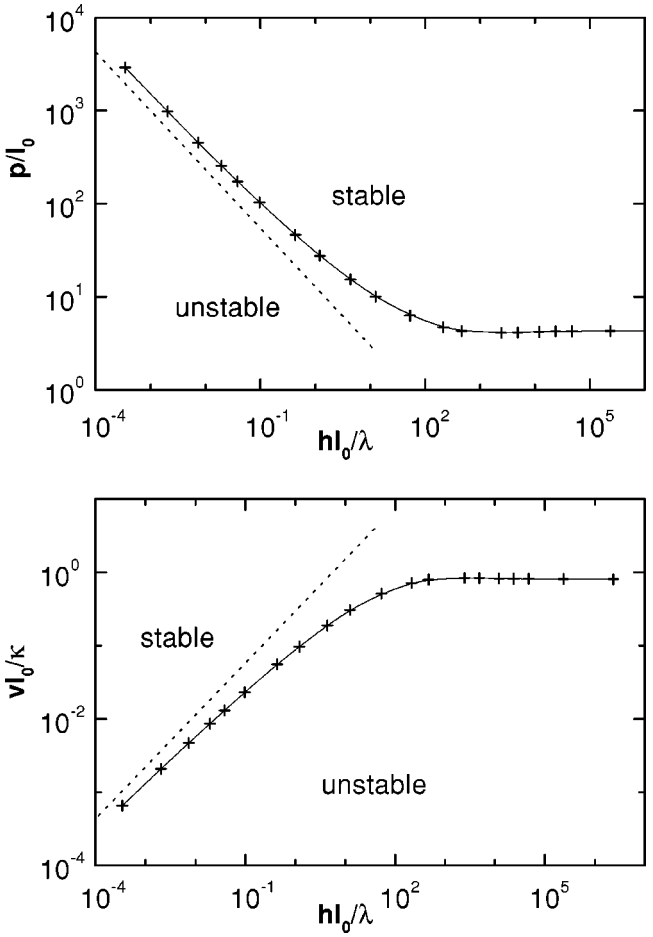

FIG. 9. Regions of stable and unstable crack spacings (top) and crack velocities (bottom) as a function of the normalized external loading parameter defined using Eq. (14). The dashed lines correspond to slopes $-2/3$ and $2/3$, respectively, in Eqs. (16). The self-driven crack array should be marginally stable.

Crack propagation should occur close to the stability limit. An argument in favor of such a marginal stability can be given when the initial phase of crack motion is considered, which precedes the formation of the stationary and uniform crack array. Initially, cracks will form on the exterior material surface. In this state, the heat loss due to the presence of the cracks is negligible, and the cracks move due to thermal stresses generated by the external cooling. Experimental and theoretical investigations of this phenomenon [1,8] demonstrate that the small cracks are initially very densely spaced (distance is of order of length). During the nonstationary phase of crack growth, the cracks experience an increasing unloading effect, which gives rise to a sequence of bifurcations in which every second crack is left behind [1,9,10]. As the length of the cracks increases, the cooling mediated by the internal crack surfaces becomes dominant, which leads to stationary, self-driven propagation of the crack array. The final crack spacing p will be attained through a sequence of bifurcations which start from a crack spacing which is much less than the critical value p_c given by the stability curve of Fig. 9 (top). According to this scenario, the crack spacing p should end up in a range $p_c < p < 2p_c$.

Figure 2 demonstrates that marginal stability can be approached also when the density of initial cracks is low. Crack branching processes reduce large initial crack spacings during the nonstationary phase.

VI. DISCUSSION AND CONCLUSIONS

The mechanism described in the preceding section selects the solution with the minimum crack spacing p and velocity among all stable solutions.

This is in contrast to the basic dynamical assumption in the model by Yakobson [12]. It selects the solution with minimal crack length L and maximal velocity. This mechanism is not present in our model based on infinite crack length (cf. Fig. 2). In [12], a one-dimensional cooling front separates fractured material from the half space containing precursor cracks. The velocity of the precursor cracks decreases when the crack length exceeds a certain finite value. Above this crack length, the cooling front can speed up by additional irregular cracking near the cooling front similar to Fig. 1. The crack spacings p are assumed to be of the order of the crack length.

In spite of these differences to our model, the predictions for the unknown quantities v and p are surprisingly similar. Our relations (16) and (17) agree with those given in [12] up to prefactors of order unity. One reason for this lies in the fact that both selection criteria require finite Péclet numbers for both small and large heat or mass transfer coefficient.

The model by Yakobson could be extended to incorporate the unloading mechanism by assuming an array of parallel precursor cracks. In such a model, three quantities must be determined, namely, the length L, spacing p, and velocity v of the precursor cracks. In addition to the crack propagation condition (6), two stability conditions are then needed. One of them must again be based on the maximum velocity assumption with respect to the crack length. The second condition follows from consideration of stability against differentiation in crack length as in thermal shock, which corresponds to Eq. (13). As a result of such an extended model we again expect that the velocity increases with p in agreement with our present model.

For a quantitative comparison between experimental results and the theoretical model better experiments are needed. They should first be conducted with larger microsphere systems without defects (grain boundaries) in order to achieve stationary propagation of parallel cracks corresponding to the present model. Measurements of crack velocity and spacing could then be compared with Eqs. (16) and (17).

Another approach is possible when the theoretical model is extended to three-dimensional tunneling cracks (Fig. 2). These cracks could again be investigated numerically by means of a stability analysis analogous to Sec. IV. However, for tunneling cracks, the spacing scales with the layer thickness, which was confirmed by experiments with different thicknesses of the layer. This is caused by the fact that a tunneling crack unloads its vicinity up to a distance comparable with the layer thickness.

ACKNOWLEDGMENTS

The authors wish to thank H. Balke, W. Pompe, and H.-J. Weiss for helpful discussions. T. B. is grateful to A. Thess for his encouragement to continue this work, and to the Deutsche Forschungsgemeinschaft for partial financial support.

APPENDIX

Here we compute the ν dependence of G according to Eq. (10). Throughout this section we use the dimensional equations. Consider the decomposition $u_i = u_i^0 + u_i^1$, $i = x,y$ of the displacement field for the crack. We demand that $u_y^0 = 0$ and $\sigma_{xy}^0 = 0$ on the entire crack line $y = 0$ and on $y = p$, i.e., the crack is absent, and solve Eqs. (2) and (3) with these boundary conditions.

The problem for u_i^1 is isothermal, and the boundary conditions are as in Fig. 4 (top) except for the stress $\sigma_{yy}^1 = -\sigma_{yy}^0$ on the crack surface $x < 0, y = 0$. Benthem and Koiter [22] find

$$G = \frac{(1-\nu^2)\sigma_0^2 p}{E} \tag{A1}$$

for constant tension σ_0 on the crack surface. By inspection of the Wiener-Hopf procedure outlined in [22] it is obvious that a nonuniform tension on the crack line will replace σ_0 in Eq. (A1) by an expression $H[\sigma_{yy}^1(x)]$, where H denotes a certain linear functional of the stress distribution $\sigma_{yy}^1(x)$. This functional is independent of ν.

We shall now show that

$$\sigma_{yy}^0(x, y=0) = \Sigma(x) E \alpha \Delta T/(1-\nu), \tag{A2}$$

where $\Sigma(x)$ depends only on the temperature distribution. By that, Eq. (10) is established. We introduce the stress function Φ by

$$\partial_y^2 \Phi = \sigma_{xx}, \quad \partial_x^2 \Phi = \sigma_{yy}, \quad \partial_x \partial_y \Phi = -\sigma_{xy}. \tag{A3}$$

The compatibility condition becomes

$$\nabla^2 \nabla^2 \Phi + \frac{\alpha E}{1-\nu} \nabla^2 T = 0. \tag{A4}$$

Two conditions on Φ are required on each boundary in order to solve this equation. The first condition is obviously $\partial_x \partial_y \Phi = 0$ on both $y = 0, y = p$.

By taking the Fourier transform of the stress-strain relations (3) with respect to x and use of the first boundary condition, it can be shown that the relation

$$\partial_y^3 \Phi + \frac{E\alpha}{1-\nu} \partial_y T = 0 \tag{A5}$$

holds on $y = 0$ and $y = p$.

The prefactor of the T derivatives in the inhomogeneous boundary condition (A5) is the same as in the differential equation (A4). The solution of the homogeneous problem for Φ can be assumed zero since stresses are purely due to thermal shrinking. The identical prefactors imply that $\Phi = E\alpha\Delta T\varphi/(1-\nu)$, where φ depends only on the temperature distribution.

[1] H.-A. Bahr, U. Bahr, and A. Petzold, Europhys. Lett. **19**, 485 (1992).
[2] O. Ronsin and B. Perrin, Europhys. Lett. **38**, 435 (1997).
[3] A. Yuse and M. Sano, Nature (London) **362**, 329 (1993).
[4] M. Marder, Phys. Rev. E **49**, R51 (1994).
[5] S. Sasa, K. Sekimoto, and H. Nakanishi, Phys. Rev. E **50**, R1733 (1994).
[6] H.-A. Bahr, A. Gerbatsch, U. Bahr, and H.-J. Weiss, Phys. Rev. E **52**, 240 (1995).
[7] M. Adda-Bedia and Y. Pomeau, Phys. Rev. E **52**, 4105 (1995).
[8] H.-A. Bahr, U. Bahr, A. Gerbatsch, I. Pflugbeil, A. Vojta, and H.-J. Weiss, in *Fracture Mechanics of Ceramics*, edited by R. C. Bradt *et al.* (Plenum Press, New York, 1996), Vol. 11, pp. 507–522.
[9] S. Nemat-Nasser, Y. Sumi, and L. M. Keer, Int. J. Solids Struct. **16**, 1017 (1980).
[10] Z. P. Bazant, H. Ohtsubo, and K. Aoh, Int. J. Fract. **15**, 443 (1979).
[11] W. Pompe, in *Thermal Shock and Thermal Fatique Behavior of Advanced Ceramics*, Vol. 241 of *NATO Advanced Study Institute, Series E: Applied Sciences*, edited by G. A. Schneider and G. Petzow (Kluwer Academic, Dordrecht 1993), pp. 3–14.
[12] B. I. Yakobson, Phys. Rev. Lett. **67**, 1590 (1991).
[13] C. Allain and L. Limat, Phys. Rev. Lett. **74**, 2981 (1995).
[14] A. T. Skjeltorp and P. Meakin, Nature (London) **335**, 424 (1988).
[15] S. Lampenscherf (unpublished).
[16] J. W. Hutchinson and Z. Suo, Adv. Appl. Mech. **29**, 63 (1992).
[17] B. A. Boley and J. H. Weiner, *Theory of Thermal Stresses* (Wiley, New York, 1960), pp. 103 and 104.
[18] *MARC K5.1 User Information* (MARC Analysis Research Corp., Palo Alto, CA, 1992).
[19] T. Boeck and U. Bahr (unpublished).
[20] Y. Wei and J. W. Hutchinson, J. Mech. Phys. Solids **45**, 1137 (1997).
[21] H.-J. Weiss (unpublished).
[22] J. P. Benthem and W. T. Koiter, in *Methods of Analysis of Crack Problems*, edited by G. C. Sih (Noordhoff International Publishing, Leyden, 1973), pp. 143–146.